energy&fuels

ARTICLE

pubs.acs.org/EF

Oil Shale as an Energy Resource in a CO_2 Constrained World: The Concept of Electricity Production with in Situ Carbon Capture

Hiren Mulchandani[†] and Adam R. Brandt[*,‡]

[†]Department of Materials Science and Engineering and [‡]Department of Energy Resources Engineering, Stanford University, Stanford, CA 94305, United States

Supporting Information

ABSTRACT: Oil shale contains large amounts of stored chemical energy: over 1 trillion barrels of oil equivalent is present in the Green River formation of the United States alone. Unfortunately, extraction of energy from oil shale generally releases significant quantities of greenhouse gases (GHGs). Liquid hydrocarbon (HC) fuels derived from oil shale have 1.2−1.75 times the fuel cycle GHG emissions of HC fuels produced from conventional oil. This paper proposes a concept that could provide transportation services from oil shale with significantly reduced carbon emissions, called electricity production with in situ carbon capture (EPICC). EPICC reduces CO_2 emissions by (1) utilizing waste heat to retort shale; (2) retorting shale beyond the point of liquid hydrocarbon production, converting much of the organic carbon in oil shale to char which is left in the subsurface; and (3) using the produced HC gas to generate electricity, which provides transportation services with no tailpipe emissions. The resulting life cycle GHG emissions from EPICC amount to ≈110 g of CO_2 per km, ≈0.5 times those of conventional fuel cycles or ≈0.33 times those from other proposed in situ oil shale conversion processes. Potential drawbacks of EPICC include uncertain operation of subsurface fuel cells, potential geophysical impacts without pressure management, and economic concerns associated with the value of stranded energy left in the formation and the long time period of retorting.

INTRODUCTION

The world resource of oil shale is nearly 3 trillion barrels (Tbbl) of oil equivalent, distributed between deposits in all regions of the world.[1] Current methods of producing energy from oil shale involve mining and retorting shale at the surface to convert kerogen to liquids and gaseous hydrocarbons (HCs). This is known as ex situ retorting. Conversion in the subsurface, or in situ retorting, is under investigation but is not likely to occur at scale for at least a decade. Methods used for in situ heating include borehole electrical heaters, electrical heating through fractures propped with conductive material, fluid heat transport through boreholes, and borehole-installed fuel cell heaters.[2]

Because of the need to address anthropogenic climate change, a major challenge for extracting energy from oil shale resources are the large greenhouse gas (GHG) emissions emitted from oil shale processing, fuel upgrading and refining, and fuel combustion. Recent work suggests that emissions from producing liquid fuels from oil shale are ≈1.25 to 1.75 times those of fuels produced from conventional oil, on a full-fuel-cycle (well-to-wheels) basis.[2−5] These emissions consist almost entirely of carbon dioxide (CO_2), with minor emissions of methane.

These emissions estimates raise a question: is the energy content of shale effectively "off limits" in a GHG constrained world, or is there a way to extract the stored chemical energy from oil shale with greatly reduced CO_2 emissions? This paper describes electricity production with in situ carbon capture (EPICC), a proposed method of providing transportation services from oil shale with greatly reduced CO_2 emissions.

GHG Emissions from Current Methods of Oil Shale Extraction. Carbon dioxide is directly emitted in all three life-cycle stages of current methods of producing and consuming liquid fuels from oil shale: (1) retorting of oil shale to generate unrefined HCs, including crude shale oil and HC gases; (2) upgrading and refining of crude shale oil to refined HC fuels; (3) combustion of refined HC fuels in vehicles.

Emissions from oil shale retorting result from (1) thermal energy requirements of retorting, (2) other energy consumption during retorting, and (3) CO_2 emitted from shale mineral matter.[4] The thermal energy demands of retorting are defined as the heat of retorting, which includes[6] (a) the heat content of shale mineral matter at the final temperature of the retorted shale; (b) the heat of reaction of kerogen decomposition; (c) the heat of reaction of mineral reactions in shale (e.g., decomposition of carbonates); (d) the heat to vaporize generated hydrocarbons and water contained in shale (both bound and free water); (e) the heat contents of gas, water, and oil vapors at the exit temperature of the retort.

Emissions of CO_2 also occur due to energy consumed in nonthermal energy requirements of retorting. For ex situ processes this includes mining the raw shale, crushing and preprocessing raw shale, and disposal of spent shale. For in situ retorting, these include energy consumed in drilling and casing wells along with other subsurface operations and surface processing.

Importantly, CO_2 is also emitted from shale mineral matter itself. This is due to both oxidation of organic carbon in the kerogen and bitumen and inorganic CO_2 released from shale mineral matter.[4] Organically derived CO_2 is emitted during retorting due to the reaction of existing oxygen with organic

Received: December 17, 2010
Revised: February 22, 2011
Published: March 11, 2011

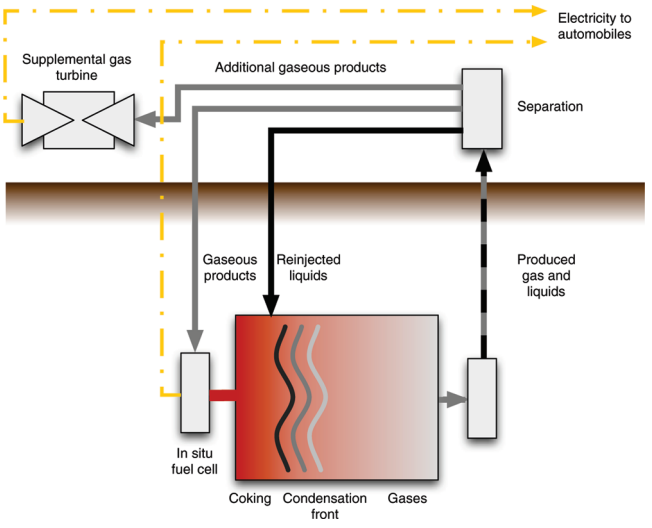

Figure 1. System diagram of EPPIC process. Electricity generation in subsurface provides the heat requirement for retorting. Separation of gaseous from liquid HCs can occur in the subsurface at a condensation front or in above ground separation with reinjection.

matter in the presence of retorting heat; this emission source is generally unavoidable during retorting and scales with the organic content of the shale rather than the mineral content of the shale. (The elemental makeup of kerogen has been measured as ≈81.7 wt % C, 10.2% H, 3.05% N, and 5.01% O.[4] This oxygen leaves kerogen during decomposition as water vapor and CO_2.) Also, CO_2 is emitted from shale due to reactions of inorganic mineral matter during retorting. These reactions include decomposition of saline minerals, such as nahcolite ($NaHCO_3$) and dawsonite [$NaAlCO_3(OH)_2$], at low temperatures. Carbonate minerals such as dolomite [$MgCa(CO_3)_2$] and calcite ($CaCO_3$) also decompose at higher temperatures. These reactions are much more problematic due to the abundance of carbonate minerals in oil shale (up to 40−50 wt %).[7] There are uncertainties about the rate and mechanisms of carbonate decomposition, which have resulted in significantly different predictions of decomposition rates by different models.[8−11]

Previous methods proposed to reduce CO_2 emissions from oil shale extraction are varied. Some suggest to use low GHG sources such as off-peak wind power,[12] nuclear power,[13] or solar power[14,15] for retorting heat requirements. Others suggest shifting from electricity-based in situ processes to processes relying on subsurface combustion for direct heating.[16,17] Lastly, some have proposed capture and storage of CO_2 emissions from ex situ retorting.[18]

EPICC and Optimization for Reduced Emissions. In EPICC, waste heat from a solid oxide fuel cell (SOFC) placed in the subsurface is transferred via conduction to a geologic formation containing oil shale (see Figure 1). Heat causes kerogen and bitumen to decompose into liquid and gaseous HCs. As vaporized liquid HCs move toward producer wells and contact cool shale, some condensation occurs (see discussion of bounding cases in the Experimental Section). Upon further heating, liquid HCs crack into low-molecular weight gases (CH_4, H_2, CO, CO_2) and char ($CH_{0.63}N_{0.056}O_{0.02}$ in primary char, $CH_{0.23}N_{0.03}O_{0.02}$ in secondary char). Separation of HC liquids and gases could also be performed at the surface, with produced liquids reinjected into the hot formation to undergo further cracking. (Such reinjection of produced liquids has been proposed by AMSO.[16] The AMSO CCR (conduction, convection, and reflux) process relies on a boiling pool of liquid oil for convective heat transfer, which may need to be replenished during retorting.) Produced HC gases are fed back into the fuel cell, generating electricity and providing more waste heat for retorting. Excess gas can be sent to a combined cycle gas turbine to produce additional electricity. EPICC is designed to maintain, to the extent possible, a bulk shale temperature below that at which significant carbonate mineral decomposition to CO_2 occurs, since this would render it impossible to produce low-CO_2 electricity. Because of the volumes of produced gases generated during retorting and cracking of HCs, EPICC is in most cases a self-fueled process.

A key factor in the efficiency and low-CO_2 nature of EPICC is the "rearrangement" of the order of the conventional transportation fuel cycle (see Table 1). The chemical energy contained in the shale is converted to work (e.g., electricity) in the subsurface, rather than in distributed internal combustion engines, allowing waste heat from work conversion to supply the heat of retorting. In other words, retorting thermal demands are provided by the waste heat that is unavoidably generated with any conversion of chemical energy to work. Also, conversion to work occurs in a centralized location, enabling easier control of resulting CO_2 emissions (although this is not explored here).

EPICC should not be viewed as a method to produce natural gas from shale: such methods would consume significant amounts of primary energy and result in a lower value product than the oil that was destroyed to produce gas. Instead, EPICC produces gas as an intermediate product, and the waste heat output from conversion of this gas to electricity provides the driving heat for kerogen decomposition and cracking of hydrocarbons. Thus, the heat integration with electricity production is a fundamental part of the EPICC concept.

EXPERIMENTAL SECTION

In order to explore the EPICC concept, we built STAN/DOS (Stanford Decomposition of Oil Shale), a model that includes all relevant chemical reactions that occur in the subsurface during retorting. STAN/DOS models oil shale reactions at the "block-level" (i.e., 1000 kg of shale). We then use STAN/DOS results to develop a first-order assessment of the energetics of implementing EPICC at scale. Because EPICC operates at significantly different temperature and time regimes than other proposed in situ conversion processes, standardized results from previous efforts could not be used to model EPICC.

Block-Level Modeling with STAN/DOS. Equations corresponding to the decomposition of nahcolite,[4] calcite,[4] dolomite,[4] bitumen,[19] and kerogen,[19] the conversion of primary[19] and secondary char,[19] and the cracking of 11 oil fractions[19] were incorporated into STAN/DOS from the literature (see the Supporting Information). All data are specific to the Green River formation of the U.S. and will be of limited applicability elsewhere, due to differing kerogen amounts and composition, H/C ratio, and inorganic mineral makeup. Reactions were considered to be either decomposition reactions (breakdown of solid mineral matter), cracking reactions (breakdown of a liquid hydrocarbon), or boiling reactions (phase change for a species). STAN/DOS was coded into MATLAB v. 7.1.[20] Stocks in STAN/DOS are cumulative and are accounted for by summing inflows and outflows:

$$S_{it} = \sum_i F_{ijt} - \sum_j F_{jit} + S_{j(t-1)} \quad (1)$$

where S_{it} represents stock of component i (in kilograms of product), F_{ijt} represents flow of reactant i to product j (in kilograms of reactant/day), F_{jit} represents flow of reactant j to product i (in kilograms of product/day),

Table 1. Conceptual Differences between Traditional Oil Shale Retorting Process and EPICC

	liquids production	EPICC
resource	chemical energy in shale	chemical energy in shale
heat source	direct thermal or electrical energy	secondary use of waste heat
energy carrier to consumer	liquid fuel	electricity
conversion to work	automobile engine	in situ fuel cell
scale of conversion to work	decentralized	centralized
waste heat from conversion	to atmosphere	to shale

and $S_{j(t-1)}$ represents stock of component j at time step $t-1$. The compositions of energy carrying species (including all forms of char) are from general retorting model of Burnham and Braun.[19]

Flows in STAN/DOS are noncumulative: a reaction occurs on a stock of the reactant, with a certain fraction of the reactant i going to produce product j:

$$F_{ijt} = S_{i(t-1)} r_{i(t-1)} f_{ij} \tag{2}$$

where F_{ijt} represents flow of reactant i to product j (in kilograms of product/day), $S_{i(t-1)}$ represents stock of component i at time step $t-1$ (in kilograms of reactant), $r_{i(t-1)}$ represents the reaction rate at time step $t-1$ (in/day), and f_{ij} represents the fraction of reactant i which flows to product j during the reaction (kilograms of j produced/kilograms of i reacted, constant based on reaction stoichiometry).

Reaction rates are modeled using first order kinetics:

$$r_{i(t-1)} = \Lambda_i \exp[-k_{i(t-1)} t] \tag{3}$$

where $r_{i^*t-1)}$ represents the reaction rate for reactant i at time $t-1$ (in/day), Λ_i is the pre-exponential factor for reactant i (in/day), $k_{i(t-1)}$ is the reaction rate constant for reactant i at time $t-1$ (in/seconds) and t is the time step (in seconds).

$k_{i(t-1)}$ is calculated according to

$$k_{i(t-1)} = \Lambda_i \exp\left[\frac{-E_{A,i}}{RT_{t-1}}\right] \tag{4}$$

where $k_{i(t\text{-}1)}$ is the reaction rate constant for reactant i at time $t-1$ (in/seconds), A_i is the pre-exponential factor for reactant i (in/day), $E_{A,i}$ is activation energy for the reaction (in Joules/mole), R is the universal gas constant (in Joule/mole Kelvin), and $T_{t\text{-}1}$ is the temperature of the reaction at time $t-1$ (in Kelvin).

The energy flux associated with a reaction is noncumulative and is determined by multiplying a stock of a species with its reaction rate and its energy demand of reaction:

$$Q_{it} = S_{i(t-1)} r_{i(t-1)} q_i \tag{5}$$

where Q_{it} is the energy flux for reactant i (in megajoule/day), $S_{i(t-1)}$ is the stock of reactant i at time t (in kilograms of reactant), $r_{i(t-1)}$ is the reaction rate for reactant i at time t (in/day), and q_i is the energy demand of the reaction.

The energy content associated with a reactant or product is cumulative and is determined by multiplying a stock of a species with its higher heating value:

$$E_{it} = q_j S_{i(t-1)} \tag{6}$$

where E_{it} is the energy content of species i at time t (in megajoule), q_j is the higher heating value for species i (in megajoule/kilogram of reactant), and $S_{i(t-1)}$ is the stock of species i at time t (in kilograms of reactant).

The electrical output from the fuel cell is determined by multiplying the efficiency of the fuel cell with the weighted energy contents of the gases used to fuel it:

$$\mathrm{FC}_{\mathrm{electricity}} = \eta\left(\sum_t \sum_i (\mathrm{mf}_i q_i x_t) + \sum_t y_t q_i\right) \tag{7}$$

where $\mathrm{FC}_{\mathrm{electricity}}$ is the electricity produced by the fuel cell (in megajoules of electricity), η is the efficiency of the fuel cell (in megajoule of electricity/megajoules of gas), mf_i is the mass fraction of each of the gases used to fuel the fuel cell (unitless), q_i is the higher heating value for species i (in megajoule/kilogram of reactant), x_t is the mass of gas extracted from the shale to fuel the fuel cell (in kilograms), and y_t is the mass of externally purchased gas used to fuel the fuel cell (in kilograms). The heat output from the fuel cell is determined by multiplying $(1-\eta)$ by the weighted energy contents of the input fuel gases.

The energy required to boil off each oil fraction is determined by multiplying the stock of each oil fraction by its enthalpy of vaporization and dividing by its molar mass:

$$\mathrm{energy}_{\mathrm{boiling\ oil}} = \sum_i S_{i(t-1)} w_i \left(\frac{1}{M_i}\right) \tag{8}$$

where $\mathrm{energy}_{\mathrm{boiling\ oil}}$ represents the energy required to boil off oil fraction i (in megajoules), $S_{i(t-1)}$ represents the stock of component i at time step $t-1$ (in kilograms of reactant), w_i represents the enthalpy of vaporization of each oil fraction (in megajoules/mole), and M_i represents the molar mass of each oil fraction (in kilogram/mole). This in turn allows for the determination of the total energy required to boil off all the oil produced from the decomposition of bitumen and kerogen in the oil shale:

$$\mathrm{energy}_{\mathrm{boiling\ oil}} = \sum_i \max(\mathrm{energy}_{\mathrm{boiling\ oil}}) \tag{9}$$

where $\mathrm{energy}_{\mathrm{boiling\ oil}}$ represents the total energy required to boil off all the oil in the shale (in megajoule) and max $\mathrm{energy}_{\mathrm{boiling\ oil}}$ represents the largest value of the energy required to boil off each oil fraction (in megajoules), as shown in eq 8.

The following assumptions were made in STAN/DOS: the starting mass of shale is 1000 kg; the energy cost associated with cleaning or preprocessing of HC gas at the surface before injecting it into the fuel cell is negligible; the effect of pressure increase on chemistry is not included due to the assumption of relatively low operating pressures through expulsion of produced HCs (see Discussion of future work below). Table 2 shows the cases examined using STAN/DOS. In all cases the heating rate applied is the ideal heating rate for the standard case.

Scale-Up Modeling Methods. In order to compare EPICC with previously proposed in situ conversion processes, we perform first-order scale up calculations and apply full-fuel-cycle (well-to-wheels) life cycle analysis to analyze all energy inputs and outputs from the process. To allow for comparison, these calculation methods are analogous to those for an analysis of the Shell in situ conversion process (ICP).[3]

The scale-up analysis uses results from the standard case STAN/DOS run outlined above. Using STAN/DOS results for a 1000 kg block, the results are scaled to a 300 m by 300 m heated area (see the Supporting Information for a plot plan). The method calculates energy and key material (e.g., steel and cement) inputs for preliminary operations, drilling, casing, and cementing of wells, freeze wall construction, site reclamation, electricity generation efficiencies, and transport of the final energy carrier to consumers. Internally to the heated block, it is assumed that decomposition reactions proceed evenly (even temperature distribution within heated zone), while thermal conduction outside of the heated area and the associated energy penalties are calculated using Fourier 1-D heat conduction (convection is neglected). All energy inputs are converted to the mass of CO_2 emissions using fuel-specific emissions factors. See the Supporting Information for more calculation details.

Table 2. Reactive Composition of Oil Shale for Different Cases Examined in STAN/DOS (wt %)[a]

	nahcolite	calcite	dolomite	bitumen	kerogen	bound water	free water
standard case	2	12	15	0.9	18	0.25	4.75
high kerogen content	2	12	15	1.25	25	0.25	4.75
low kerogen content	2	12	15	0.5	10	0.25	4.75
high water content	2	12	15	0.9	18	0.5	9.5
low water content	2	12	15	0.9	18	0.125	2.375

[a] Remainder of mass is inert mineral matter.

The differences between EPICC scale-up analysis and the previous ICP analysis include (1) increased retorting time (2000 days) in EPICC to allow low temperature retorting and therefore avoid decomposition of carbonate minerals; (2) condensation and reinjection of produced liquid HCs, with additional energy burdens; and (3) the use of an auxiliary gas turbine to generate electricity on site from excess produced gas (beyond that needed in the fuel cell to produce heat for reaction).

All energy required to initially fuel the system is assumed provided by a previously operated EPICC installation (e.g., a steady-state assumption). In practice, the first EPICC project in an area would be fueled with purchased natural gas, and extraneous HC gas production from the end of that operating facility could be used to fuel the next installation. The CO_2 implications of this are minimal, as the weighted CO_2 intensity of EPICC outputs is 51.5 g of CO_2/MJ HHV (base case) virtually identical to natural gas CO_2 intensity.

Importantly, the potential for subsurface separation of liquid and gaseous HCs cannot be studied using the STAN/DOS model of a single shale block, so we perform bounding case calculations to assess the impacts. The energy required to boil off all liquid HCs produced from shale is 30.2 MJ/t (HC enthalpy of vaporization, weighted by product distribution). Assuming surface condensation is required, it is assumed that the oils boils off and is reinjected 1 time (low case) to 5 times (high case) to allow additional cracking in the subsurface. This will result in 30−151 MJ lost, assuming warm liquids reinjection and loss of the heat of vaporization as waste heat: this is 0.4−1.9% of the total energy content of the oil shale; therefore, boiling is not likely to be a significant energy drain in EPICC. The energy cost of reinjection of the liquids is similarly small in magnitude.

Conversion of produced gases to electricity is assumed to occur in the subsurface SOFC (η = 47% HHV basis) or in an auxiliary gas turbine (η = 50% HHV basis). Transmission of electricity to consumers is assumed to suffer 8% transmission and distribution losses. To ensure fair comparison with the ICP, which includes steel and cement casing embodied energy inputs, embodied energy in subsurface SOFCs is assessed. At required heat input rates and expected retorting times (2−3 years of heating), average per-tonne power output from subsurface SOFCs amounts to 15−23 W/t. Embodied energy in SOFCs (planar fuel cell elements plus balance of system components) is approximately 150 MJ per kW SOFC capacity.[21] Thus, embodied energy inputs to SOFCs equal ≈3−4 MJ/t or ≈0.1% of total energy inputs to the system.

Electricity is assumed consumed in a Nissan Leaf electric car, using U. S. federal (CAFE) efficiency estimates of 34 kWh per 100 miles. (There is some uncertainty about the Nissan Leaf range: Nissan claims 100 mile range per charge (http://www.nissanusa.com/leaf-electric-car/), but stricter EPA driving tests (using auxiliary loads such as heaters and radio) resulted in a 73 mile range per charge.) In order to compare to the ICP, the Honda Fit was chosen as a similarly sized compact car powered by an internal combustion engine (35 mpg highway). These fuel efficiencies are equivalent to 0.435 km/MJ for the gasoline-powered car and 1.323 km/MJ for the electric car.

Metrics of System Impacts. The block-level carbon intensity of retorting is determined by dividing the mass of CO_2 leaving the shale and the mass of CO_2 produced during complete oxidation of the gases used in the fuel cell, by the total electrical energy output from the fuel cell:

$$\Psi = \frac{\sum_t c_t + \sum_t d_t}{\sum_t l_t} \quad (10)$$

where ψ is the carbon intensity in (grams of CO_2/megajoules of electricity), c_t is the mass of CO_2 leaving the shale, summed over the length of the entire process (in grams of CO_2), d_t is the mass of CO_2 produced during complete oxidation of the gases used in the fuel cell, summed over the length of the entire process (in grams of CO_2), and l_t is the energy associated with the electricity produced by the fuel cell, summed over the length of the entire process in (megajoules of electricity).

To these block-level retorting emissions calculated in STAN/DOS, GHG emissions from all other life cycle process stages are added. These are calculated by multiplying energy consumption in processes (e.g., drilling) by the fuel-specific emissions factor for the fuel consumed in that process (e.g., drilling consumes diesel with emissions of 77 g of CO_2/MJ).[22]

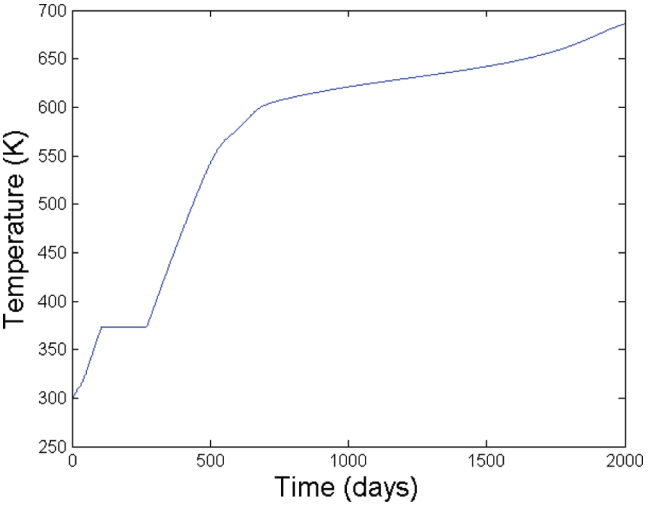

Figure 2. Temperature (K) vs time (days) for standard case.

RESULTS

Block-Level Modeling. Figure 2 shows the temperature profile generated during operation of STAN/DOS in the standard case. At a temperature of 373 K, the bound water in the system starts to boil, causing the temperature to remain constant. Once the water has boiled off, the temperature starts to rise again until it reaches approximately 625 K, at which point oil cracking reactions absorb significant amounts of thermal energy, causing the temperature rise to be less steep. At the end of the process,

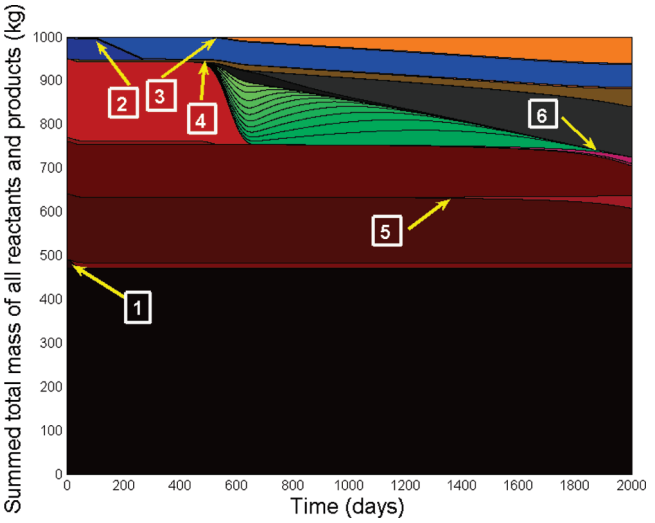

Figure 3. Summed total mass of all reactants and products (kilograms) vs time (days) for the standard case.

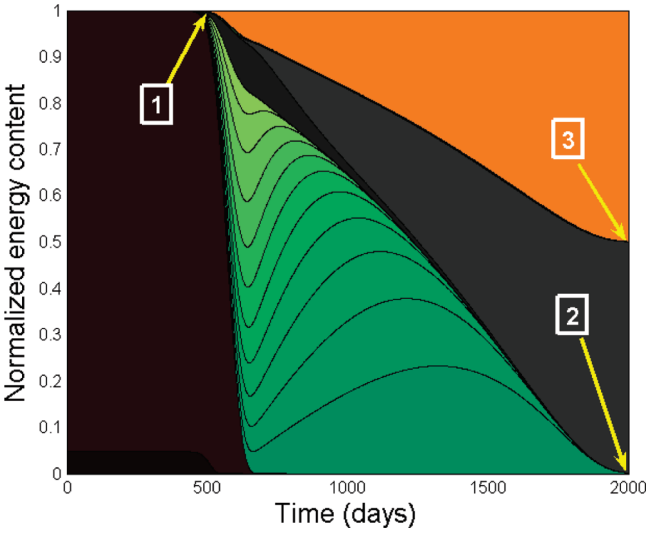

Figure 4. Normalized summed total energy content of bitumen, kerogen, oil fractions, char, and gases vs time (days) for the standard case.

the temperature is still rising, although the final value attained is approximately 680 K.

Figure 3 shows the mass balance profile generated during operation of STAN/DOS under standard conditions (see Figure 5 for the mass balance color key). Mass conservation is maintained during the process. The following features are observed: (1) nahcolite starts to decompose to generate Na_2CO_3 and CO_2; (2) onset of bound and free water boiling; (3) H_2, CO, and CH_4 gas start to be generated in sufficient quantities to allow for these gases to be removed for operation of the geothermic SOFC; (4) bitumen and kerogen start to decompose to oil, gas, and char. The oil is composed of 11 fractions. Each fraction subsequently decomposes to give lighter oil, gases, and char until all of the oil is cracked; (5) decomposition of dolomite results in production of MgO, $CaCO_3$, and CO_2; and (6) oil cracking is complete.

Figure 4 shows the energy balance generated during operation of STAN/DOS under standard conditions (see Figure 5 for energy balance color key). The following features are observed:

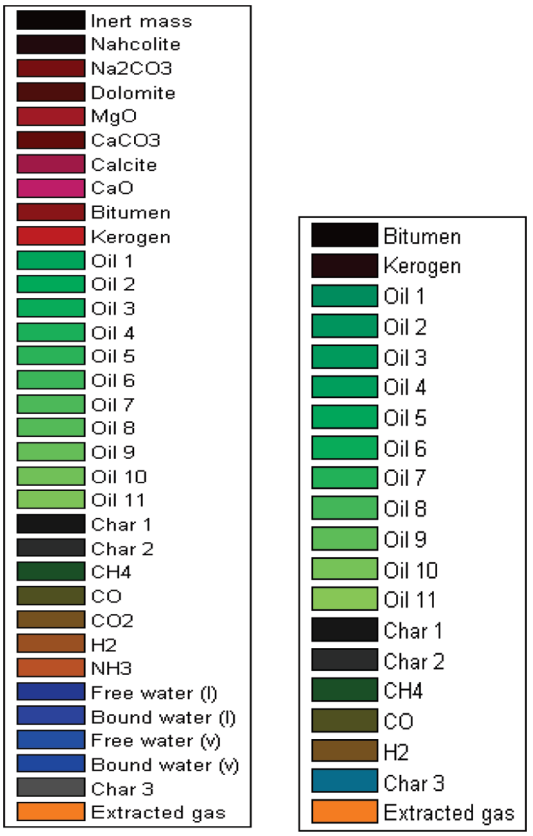

Figure 5. Legend for mass balance (left) and energy balance (right) plots.

(1) The energy content of bitumen and kerogen starts to be divided up among the oil fractions, char, and gases, as both bitumen and kerogen undergo decomposition; (2) primary char stops decomposing; (3) secondary char stops decomposing. The amount of energy left over in secondary char is greater than that removed to self-fuel the fuel cell and run the auxiliary gas turbine. Because the cracking of oil is complete by the end of the process, much of the energy (~50%) from the bitumen and kerogen has gone to produce useful gas products which are withdrawn from the subsurface to fuel the process.

Table 3 shows the energy contents and extraction efficiency for the different cases examined in STAN/DOS. Note that because of the differences in conditions for alternative cases, applying the standard case heating regime overheats some scenarios (e.g., low kerogen, low water), while leaving significant energy behind in other cases (e.g., high kerogen). Because of the diversity of shale makeup by the formation layer (porosity, richness, etc.), a heating plan based on the standard case makeup would result in somewhat uneven conversion across a diverse shale formation.

Scale-Up Modeling. The resulting life-cycle energy flows into and out of a full scale EPICC implementation are presented in Table 4. These results are the average of the low and high oil boiling bounding cases described above, applied to the standard shale makeup case. These results are compared to results from the ICP to allow comparison of overall energy flows and CO_2 emissions. Results from the ICP are the average of high and low cases from previous analysis,[3] with minor improvements to reclamation energy inputs and other stages (see the Supporting Information).

Table 3. Energy Contents and Extraction Efficiency for All Cases Considered (megajoule/tonne)

case	initial energy content	extracted energy	energy left behind	extraction eff. (%)
standard	7 806	3 454	4 352	44.2
high kerogen	10 841	4 047	6 795	37.3
low kerogen	4 337	1 922	2 415	44.3
high water	7 806	3 313	4 493	42.4
low water	7 806	3 458	4 347	44.3

While total energy outputs from the EPICC system are ≈55% of the total energy outputs from ICP, the final energy output is in the form of electricity. Given the much more efficient conversion of electricity to transportation serves in BEVs compared to IC engines, the transportation services supplied by EPICC are ≈65% larger per tonne of shale retorted (1630 km vs 990 km per tonne of shale retorted, see Table 5).

Importantly, CO_2 emissions per unit of transportation services supplied are significantly lower for EPICC than in the ICP. Table 5 shows that EPICC has lower CO_2 emissions per unit of transportation services provided compared to the ICP and conventional oil. The CO_2 intensity of transport powered by EPICC (in grams of CO_2/kilometer) approaches, but does not reach, the CO_2 intensity of electric transport powered by natural gas. EPICC CO_2 intensity is somewhat higher than a pure natural gas system due to balance-of-system consumption (drilling, freeze wall) and minor amounts of carbonate decomposition and other mineral CO_2 sources.

Some of the GHG benefit of EPICC derives from the use of in situ fuel cells, while some of the benefit results from in situ coking of kerogen to char. In order to ensure a consistent comparison to the ICP, an ICP case fueled with fuel cell heaters is also included in Table 5. As can be seen, an ICP with fuel cell heaters has significant electricity exports, even after powering onsite usage such as the freeze wall and reclamation pumping and treatment. CO_2 emissions per kilometer for the ICP with fuel cell heaters are lower than conventional oil but not as low as EPICC (i.e., 183 g of CO_2/km vs 111 g of CO_2/km).

Lastly, since EPICC produces electricity instead of liquid fuels, comparison can be made between EPICC CO_2 emissions per unit of power produced and other electricity sources (see Table 6). As can be seen, EPICC produces emissions somewhat greater than a NGCC system in the base case. High case emissions from EPICC (taken from the low kerogen case) reflect high rates of carbonate decomposition, pushing CO_2 emissions to levels comparable to coal-fired power plants (and potentially higher if very high temperature SOFCs are used). In order to allow comparison with other fossil energy sources, an EPICC case with carbon capture and storage (CCS) is calculated, using IPCC CCS data (see Table 6).

DISCUSSION

As Table 3 shows, the fraction of shale energy content extracted for the standard case is ≈44%, with a range depending on shale characteristics of 37−44%. This is significantly lower than the 70+% of the initial energy content extracted with in situ and ex situ technologies. Also, the heat inputs to retorting in EPICC are significantly larger than the ICP (Table 4), due to the heat requirements for oil cracking and thermal demands of reheating oil reinjected after condensation (see Table 4). These disadvantages are mitigated by the profound benefits of utilization of waste heat for retorting.

Table 4. Comparison Results for EPICC and ICP Implementation at Scale

	EPICC		ICP		notes
	inputs	outputs	inputs	outputs	
miscellaneous	39		36		
drilling	10		10		
freeze wall	64		43		
retorting inputs					
primary energy cons.	2956		1060		*a*
delivered retorting heat	1566		530		
electricity	0		530		
waste heat	1566		0		
retorting outputs					
oil		0		2587	
gas		498		0	*b*
electricity		1389		0	
auxiliary elec. prod.	498	249	0	0	
reclamation	134		134		*c*
offsite energy output		1437		2587	*d*
electricity transport	115				*e*
electricity to consumer		1322			
refining			70	2404	*f*
transport (crude + refined)			19		
refined fuel to consumer				2404	*g*
total energy to consumer	1322 MJ electricity		2404 MJ gasoline		

[a] EPICC equals total gas inputs to subsurface fuel cell, which produces 1209 MJ electricity and 1363 MJ heat. ICP equals primary energy input to the turbine for electricity generation for retorting. [b] Total produced gas for EPICC is 2572 + 537 MJ, of which 2572 is recycled back into fuel cell for primary retorting energy supply. Produced gas for ICP is 1006 MJ, which is entirely fed back into the system for electricity generation, so it is not reported as an output here. [c] For ICP, reclamation energy is larger than that reported in earlier analysis. Earlier analysis only included energy inputs to pumping, not treatment of reclaimed water. This assessment includes treatment energy for 20 pore volumes of reclamation flushing water, see the Supporting Information. [d] For EPICC, equals total electricity generation, less self-consumption of process stages that consume electricity: pumping, freeze wall, reclamation, and other minor uses. [e] For the EPICC case, 8% transmission and distribution losses are included from on site electricity to electricity to consumer. [f] Refining energy is supplied externally (70 MJ) plus internal consumption and loss (difference between 2587.4 and 2403.9 MJ). See Brandt[3] for details of the refining model. [g] For ICP, refined oil product transport is changed from the previous work[3] to equal intensity used in the GREET model.

Importantly, the great majority of the original carbon mass is left behind in the formation. In the standard case, 189 kg of kerogen and bitumen per tonne contains 155.5 kg of C. The remaining char (primary and secondary char) after production equals 115.2 kg, containing 106.5 kg of C (nearly all char is converted to secondary char through heating). Thus, the carbon retention rate in the subsurface is ≈68%. This can be compared to a carbon retention rate of less than 30−40% in the ICP due to stranded char and oil remaining in the subsurface.

Table 5. Life-Cycle GHG Emissions from Passenger Transport Using Conventional Oil, Two ICP Implementations, and EPICC

	ICP	ICP w/fuel cell heaters	EPICC	conventional oil	
electricity delivered to consumer [MJ/t shale]		326	1322		
gasoline delivered to consumer [MJ/t shale]	2404	2404			
distance traveled [km/t shale]	1046	1449	1633		
upstream CO_2 emissions [kg CO_2/t shale]	147.8	88.0	147.0		*a*
vehicle CO_2 emissions from consuming energy [kg CO_2/t shale]	177.4	177.4	0		
weighted life cycle emissions [g CO_2/MJ]	135.3	97.2	111.2	95	*b,c*
tailpipe emissions [g CO_2/km]	169.6	122.4	0.0	169.5	
life cycle CO_2 intensity of travel [g CO_2/km]	310.8	183.1	111.2	218.2	*c,d*

[a] This value for the ICP is somewhat higher than Brandt[3] due to the inclusion of noncombustion (e.g., kerogen-derived CO_2 emissions during retorting). This factor equals ~2.5 g of CO_2/MJ. [b] Conventional gasoline blendstock is assumed to have emissions of 95 g of CO_2/MJ, a typical value from full-fuel-cycle models (e.g., GREET or GHGenius) [c] This weighted average is an even weighting of gasoline and electricity on a per-megajoule basis. This is a less useful indicator due to the much higher utility of electricity in transport. A more useful indicator when comparing gasoline and electricity-based systems is grams of CO_2/kilometer. [d] Modeled energy consumption factors are for two small cars of comparable size. BEV: Nissan Leaf electric vehicle (34 kWh/100 mi range average energy consumption). ICV: Honda Fit, EPA rating 33 mpg. These prorate to 1.32 km/MJ electricity (Leaf) and 0.435 km/MJ (Fit).

Table 6. GHG Emissions from EPICC Compared to Other Electricity Sources, With and Without Carbon Capture and Storage (CCS)

	CO_2 intensity [kg of CO_2/MWh]	range [kg of CO_2/MWh]	source/ notes
coal - typical U.S.	1075		22, *a*
coal - new pulverized coal	762	736− 811	*b*
coal - PC + CCS	112	92−145	23, *b*
natural gas combined cycle (NGCC)	367	344−379	23*b*
NGCC + CCS	52	40−66	23,*b*
EPICC	400	344−675	*c*
EPICC w/CCS	59	51−99	*d*

[a] Typical coal plant emissions assumes 89.75 g of CO_2/MJ HHV coal CO_2 intensity and 30% efficiency, HHV basis. [b] IPCC based value is representative value, sourced from Table 8.1. Range is low, high range from same table. [c] EPICC midrange case is the standard case CO_2 intensity for process gas (accounting for conversion efficiency of SOFCs) plus additional emissions from shale organic and mineral matter. Low − high range is from high kerogen case (low) and high kerogen case (high). [d] CCS implementation assumes net capture rate of 85.3%, the same reduction assumed for coal (PC + CCS) in IPCC reports.

At realistic electricity and oil prices and characteristic heat contents (75 $/bbl, 6.1 GJ/bbl, 0.08 $/kWh), offsite energy outputs (per tonne of shale treated) from EPICC are approximately equal in value to those from the ICP but only ≈80% of those from an ICP implementation with fuel cell (see Table 5). Therefore, EPICC would be unlikely to be implemented in a non-CO_2 constrained world because a similar capital investment in wells and fuel cells would allow higher profits with an ICP-like arrangement (larger revenues, faster return on investment). However, if the cost of CO_2 emissions credits is $50/t of CO_2, net revenues per tonne of shale treated are approximately equal for EPICC and ICP with fuel cell heaters and much higher than conventional ICP (revenues calculated as above less carbon tax calculated using kg of CO_2 emissions from Table 5). In high carbon tax scenarios, EPICC could represent an economic improvement over traditional in situ retorting as well as an environmental improvement. This is particularly true because the magnitude of processing flows is not significantly different in EPICC than the ICP, as compared to low-CO_2 oil shale production schemes with significant additional capital investment required for carbon dioxide capture and storage.

What is more questionable is whether EPICC would be economically valuable in a high carbon tax scenario compared to low-carbon renewable energy technologies (e.g., the higher carbon prices that tip the balance toward EPICC and away from the ICP would also disfavor carbon-based fuels in general). Also, EPICC should be considered relative to the variety of other low-CO_2 oil shale technologies that have been proposed. These technologies include nuclear powered oil shale retorting, oil shale retorting with intermittent wind power, and oil shale retorting with CCS.[4] These technologies will have CO_2 emissions similar to that of conventional oil and could be less costly than EPICC.

There are a number of challenges associated with implementing EPICC in a real-world setting. These include (1) effective and reliable operation of a subsurface SOFC, (2) effective subsurface separation of gaseous hydrocarbons from those that are in the liquid phase at standard temperature and pressure, (3) subsurface stresses associated with generating large volumes of gaseous products, (4) economic factors such as the cost of leaving energy in the subsurface or the long time of retorting; and (5) the other environmental difficulties associated with in situ oil shale extraction.

Effective and reliable operation of a subsurface SOFC is not certain, given the relatively advanced technology involved and the potentially harsh conditions found in the subsurface. Independent Energy Partners[24−26] has been developing the geothermic fuel cell concept for use in in situ oil shale retorting. The advantages of the technology include its relatively robust nature compared to other fuel cells and its ability to utilize a variety of input HCs. The high required operating temperatures of SOFCs, a disadvantage at the surface, acts in favor of the technology in the subsurface: operating temperatures of SOFCs range from 600 to 1000 °C, more than sufficient to drive heat into the formation even at the highest retorting temperature achieved.[27] A concern is whether conductive heat transfer from the fuel cell through the well casing will be sufficiently rapid and consistent to prevent damage to the device.

Also, these operating temperatures imply high near-wellbore temperatures with a potential for associated local carbonate

decomposition (especially at the high end of SOFC operating range). The above modeling results show that at reasonable bulk shale decomposition temperatures (assuming even temperature distribution throughout shale mass), carbonate decomposition rates are limited because the kinetics of oil cracking are faster than the kinetics of carbonate decomposition. However, cases with high decomposition rates (such as the low kerogen case) imply that carbonate decomposition could be significant near the wellbore (where heat inputs relative to retorting demands are high). Future modeling using reactive multiphase flow simulators could be used to estimate the extent of heating and the significance of mineral decomposition on overall process energy consumption and CO_2 emissions.

Ideally, separation of low-carbon fuel gases from heavier HCs would occur in the subsurface, with heavy HCs remaining trapped in the formation until cracking is complete. At reservoir temperatures and pressures, most of the flowing product will be in the gas phase. Therefore, subsurface separation of heavy HCs through condensation will require a "thermal sieve" or a layer of cool rock between heaters and producers. Condensing fronts have been observed outside of the heated area in results from Shell's modeling.[28] Whether such a thermal sieve will hold up under operating conditions depends on the geometry of the operation, the permeability of the rock matrix (both natural and artificially generated during retorting), and the thermophysical properties of the system (the heat capacity of the rock, thermal conductivity of rock, latent heat of vaporization of heavier HC products). Next steps must include flow simulation modeling of the system to understand the stability of this condensing front and the potential for permeability reduction due to coking.

Additionally, potentially high subsurface pressures are a concern. The temperature increase above that reported by Shell for the ICP is modest[29] with peak temperatures reached in our slow retorting scenarios of 650 K. This will likely not induce any significant problems beyond those seen in the ICP. However, the additional increase in vapor-phase product would result in greatly increased pressures in a closed system (e.g., if vapors are not removed by production wells). The observed pressure increase will depend on the rate of product removal compared to the rate of vaporization of new products. If a condensation front holds during retorting, vapor phase HCs will be removed rapidly through condensation of heavy HCs (with attendant volumetric shrinkage) and removal of light HCs, CO, and CO_2. If a condensation front cannot be maintained, then it would likely be necessary to produce a mixed HC stream in order to keep reservoir pressures to acceptable levels. This would require surface separation and reinjection of heavy HCs, with the attendant inefficiencies.

Fourth, there are economic concerns with the opportunity cost of leaving large amounts of carbon in the ground. Since only 45% of the energy content of the shale is removed from the system in EPICC, it is not clear that profit seeking operations would leave the carbon (with economic value) in the subsurface unless a large carbon tax is applied. Additionally, the time value of money will have an impact: the required retorting times in our modeled cases are 3 times longer than the ICP, which would erode the NPV of project outputs. Whether this type of operation would be economic depends most sensitively on future carbon prices, electricity prices, and the cost of operating the subsurface fuel cells. Further exploration should be performed on the regimes of carbon prices and capital costs that would favor implementation of EPICC over a liquid fuels production operation like the ICP.

Lastly, the other environmental difficulties associated with oil shale extraction are not addressed by EPICC. These include water usage, potential aquifer impacts (salinity or contamination), and landscape impact associated with development. Whether these impacts can be reliably addressed will have a strong impact on our ability to access the useful energy contained in shale, whether through low-CO_2 means or conventional methods.

■ ASSOCIATED CONTENT

Supporting Information. Additional results from STAN/DOS model runs, as described in Table 2; additional model chemistry data inputs; and additional information on expansion of EPICC concept to large-scale implementation. This material is available free of charge via the Internet at http://pubs.acs.org.

■ AUTHOR INFORMATION

Corresponding Author

*Mailing address: Department of Energy Resources Engineering, 065 Green Earth Sciences, 367 Panama St., Stanford, CA 94305-2220. E-mail: abrandt@stanford.edu. Fax: +1 650 725 2099.

■ ACKNOWLEDGMENT

This research was performed as part of H. Mulchandani's M.S. studies at Stanford University and was funded by a Fulbright Graduate Award administered by the New Zealand Ministry of Research, Science and Technology as well as the Center for Oil Shale Technology and Research at the Colorado School of Mines. Conversations and feedback from Jeremy Boak, Marshall Savage, and Alan Burnham were instrumental in developing the concepts outlined in this paper.

■ REFERENCES

(1) Dyni, J. R. *Geology and Resources of Some World Oil-Shale Deposits*; 2005-5294; U.S. Geological Survey: Reston, VA, 2006; p 42.

(2) Brandt, A. R. Converting Oil Shale to Liquid Fuels with the Alberta Taciuk Processor: Energy Inputs and Greenhouse Gas Emissions. *Energy Fuels* **2009**, *23* (12), 6253–6258.

(3) Brandt, A. R. Converting oil shale to liquid fuels: Energy inputs and greenhouse gas emissions of the Shell in situ conversion process. *Environ. Sci. Technol.* **2008**, *42* (19), 7489–7495.

(4) Brandt, A. R.; Boak, J.; Burnham, A. K., Carbon dioxide emissions from oil shale derived liquid fuels. In *Oil Shale: A Solution to the Liquid Fuels Dilemma*; Ogunsola, O., Ed. American Chemical Society: Washington, DC, 2010; in press.

(5) Burnham, A. K.; McConaghy, J. R. Comparison of the acceptability of various oil shale processes. In *26th Oil Shale Symposium*, Golden CO, 2006.

(6) Hendrickson, T. A. *Synthetic Fuels Data Handbook*; Cameron Engineers, Inc.: Denver, CO, 1975.

(7) Camp, D. W. Oil shale heat capacity relations and heats of pyrolysis and dehydration. *Twentieth Oil Shale Symposium*, Colorado School of Mines, Gary, J. H., Ed.; Colorado School of Mines Press: Golden, CO, August 1987; pp 130−144.

(8) Campbell, J. H.; Burnham, A. K. Oil shale retorting: Kinetics of the decomposition of carbonate minerals and subsequent reaction of CO2 with char. *11th Oil Shale Symposium Proceedings*, 1978; pp 242−259.

(9) Huss, E. B.; Burnham, A. K. Gas evolution during pyrolysis of various Colorado oil shales. *Fuel* **1981**, *61* (December), 1188–1196.
(10) Thorsness, C. B. Modeling study of carbonate decomposition in LLNL's 4TU pilot oil shale retort; UCRL-ID-118677; Lawrence Livermore National Laboratory: Livermore, CA, October 14, 1994; p 27.
(11) Campbell, J. H. *The Kinetics of Decomposition of Colorado Oil Shale II: Carbonate Minerals*; UCRL-52089, Part 2; Lawrence Livermore National Laboratory: Livermore, CA, March 13, 1978; p 53.
(12) Bridges, J. E. Wind power energy storage for in situ shale oil recovery with minimal CO2 emissions. *IEEE Trans. Energy Convers.* **2007**, *22* (1), 103–109.
(13) Forsberg, C. Nuclear energy for a low-carbon-dioxide-emission transportation system with liquid fuels. *Nucl. Technol.* **2008**, *164* (December), 348–367.
(14) Berger, R.; Fletcher, E. A. Extracting oil from shale using solar energy. *Energy* **1988**, *13* (1), 13–23.
(15) Burnham, A. K. On solar thermal processing and retorting of oil shale. *Energy* **1989**, *14* (10), 667–674.
(16) Burnham, A. K. In Progress on AMSO's RD&D pilot test program. *30th Oil Shale Symposium*, Golden, CO, October 18−20, 2010, Colorado School of Mines: Golden, CO, 2010.
(17) Day, R.; P., L.; Burnham, A. K.; Vawter, G.; Wallman, H.; Harris, G.; Hardy, M. The EGL Oil Shale Project. In *27th Oil Shale Symposium*, Boak, J., Ed.; Colorado School of Mines: Golden, CO, 2007.
(18) Hatfield, K. E.; Smoot, L. D.; Coates, R. L. Near-zero CO2 emissions from the clean, shale-oil surface (C-SOS) process. In *28th Oil Shale Symposium*, Colorado School of Mines: Golden, CO, 2008.
(19) Burnham, A. K.; Braun, R. L. General kinetic model of oil shale pyrolysis. *In Situ* **1985**, *9* (1), 1–23.
(20) MathWorks. *MATLAB*, version 7.1; MathWorks: Natick, MA, 2007.
(21) Baratto, F.; Diwekar, U. Life cycle assessment of fuel cell-based APUs. *J. Power Sources* **2005**, *139* (1−2), 188–196.
(22) EIA. Carbon dioxide emissions factors; Energy Information Administration: Washington, DC, 2006.
(23) IPCC. Special report on carbon dioxide capture and storage; Cambridge University Press: Cambridge, U.K., 2005.
(24) IEP, Independent Energy Partners. Unconventional Oil Resources and Technology; Denver, CO, 2009.
(25) Savage, M. T. Apparatus and method for heating subterranean formations using fuel cells. U.S. Patent 6684948, 2004.
(26) Savage, M. T. Linearly scalable geothermic fuel cells. U.S. Patent 7182132, 2007.
(27) Lisbona, P.; Corradetti, A.; Bove, R.; Lunghi, P. Analysis of a solid oxide fuel cell system for combined heat and power applications under non-nominal conditions. *Electrochim. Acta* **2007**, *53* (4), 1920–1930.
(28) Shell. Designated mining operation reclamation permit application for the Shell Frontier Oil and Gas Inc., Oil Shale Test Project. Inc.: Denver, CO, 2007.
(29) Shell. Oil Shale Test Project, Oil Shale Research and Development Project. In Plan of Operation, submitted to Bureau of Land Management, Shell Frontier Oil and Gas Inc.: Denver, CO, 2006.